



Supramolecular Aptamers on Graphene Oxide for Efficient Inhibition of Thrombin Activity

Ting-Xuan Lin¹, Pei-Xin Lai¹, Ju-Yi Mao^{1,2,3}, Han-Wei Chu¹, Binesh Unnikrishnan¹, Anisha Anand¹ and Chih-Ching Huang^{1,4,5*}

¹ Department of Bioscience and Biotechnology, National Taiwan Ocean University, Keelung, Taiwan, ² Doctoral Degree Program in Marine Biotechnology, National Taiwan Ocean University, Keelung, Taiwan, ³ Doctoral Degree Program in Marine Biotechnology, Academia Sinica, Taipei, Taiwan, ⁴ Center of Excellence for the Oceans, National Taiwan Ocean University, Keelung, Taiwan, ⁵ School of Pharmacy, College of Pharmacy, Kaohsiung Medical University, Kaohsiung, Taiwan

OPEN ACCESS

Edited by:

Xiaomin Li,
Fudan University, China

Reviewed by:

Wei Luo,
Donghua University, China
Peiyuan Wang,
Fujian Institute of Research on the
Structure of Matter (CAS), China

*Correspondence:

Chih-Ching Huang
huangcing@ntou.edu.tw

Specialty section:

This article was submitted to
Nanoscience,
a section of the journal
Frontiers in Chemistry

Received: 16 October 2018

Accepted: 05 April 2019

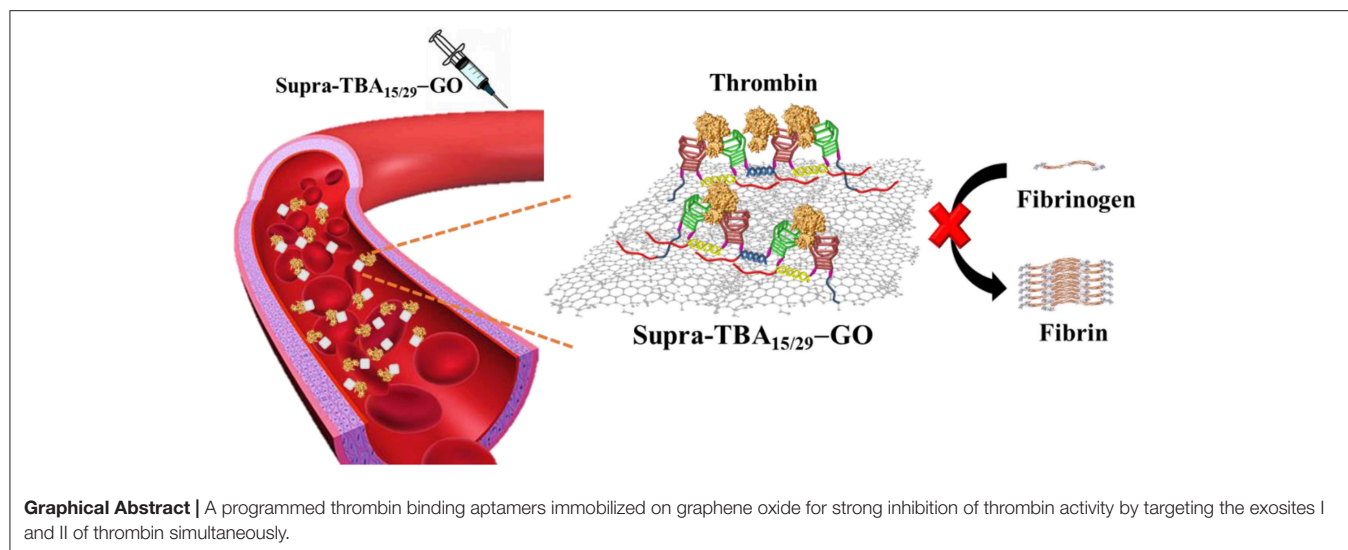
Published: 16 May 2019

Citation:

Lin T-X, Lai P-X, Mao J-Y, Chu H-W,
Unnikrishnan B, Anand A and
Huang C-C (2019) Supramolecular
Aptamers on Graphene Oxide for
Efficient Inhibition of Thrombin Activity.
Front. Chem. 7:280.
doi: 10.3389/fchem.2019.00280

Graphene oxide (GO), a two-dimensional material with a high aspect ratio and polar functional groups, can physically adsorb single-strand DNA through different types of interactions, such as hydrogen bonding and π - π stacking, making it an attractive nanocarrier for nucleic acids. In this work, we demonstrate a strategy to target exosites I and II of thrombin simultaneously by using programmed hybrid-aptamers for enhanced anticoagulation efficiency and stability. The targeting ligand is denoted as Supra-TBA_{15/29} (supramolecular TBA_{15/29}), containing TBA₁₅ (a 15-base nucleotide, targeting exosite I of thrombin) and TBA₂₉ (a 29-base nucleotide, targeting exosite II of thrombin), and it is designed to allow consecutive hybridization of TBA₁₅ and TBA₂₉ to form a network of TBAs (i.e., supra-TBA_{15/29}). The programmed hybrid-aptamers (Supra-TBA_{15/29}) were self-assembled on GO to further boost anticoagulation activity by inhibiting thrombin activity, and thus suppress the thrombin-induced fibrin formation from fibrinogen. The Supra-TBA_{15/29}-GO composite was formed mainly through multivalent interaction between poly(adenine) from Supra-TBA_{15/29} and GO. We controlled the assembly of Supra-TBA_{15/29} on GO by regulating the preparation temperature and the concentration ratio of Supra-TBA_{15/29} to GO to optimize the distance between TBA₁₅ and TBA₂₉ units, aptamer density, and aptamer orientation on the GO surfaces. The dose-dependent thrombin clotting time (TCT) delay caused by Supra-TBA_{15/29}-GO was > 10 times longer than that of common anticoagulant drugs including heparin, argatroban, hirudin, and warfarin. Supra-TBA_{15/29}-GO exhibits high biocompatibility, which has been proved by *in vitro* cytotoxicity and hemolysis assays. In addition, the thromboelastography of whole-blood coagulation and rat-tail bleeding assays indicate the anticoagulation ability of Supra-TBA_{15/29}-GO is superior to the most widely used anticoagulant (heparin). Our highly biocompatible Supra-TBA_{15/29}-GO with strong multivalent interaction with thrombin [dissociation constant (K_d) = 1.9×10^{-11} M] shows great potential as an effective direct thrombin inhibitor for the treatment of hemostatic disorders.

Keywords: thrombin, aptamer, graphene oxide, self-assembly, anticoagulation



INTRODUCTION

Stable and uninterrupted blood flow is important for maintaining a healthy life style. The human body has highly efficient bi-directional regulation of coagulation and hemolysis to prevent excessive blood flow out of injured wounds by forming clots and breaking down the clot when not needed (Doolittle, 2016; Rana and Neeves, 2016). In general, artificial triggering of blood coagulation processes is not needed, except in congenital hemophilia patients who lack factor VIII or factor IX, which can be treated by blood transfusion or injection of clotting factor (Morfini et al., 2013). On the contrary, many diseases are caused by the formation of thrombus (Previtali et al., 2011; Otsuka et al., 2016). Currently, predicting the exact place of thrombus formation in the body is difficult. So, when symptoms arise, serious issues tend to follow, which cause hemorrhage and ischemic necrosis of tissue/organs (Previtali et al., 2011; Suppiej et al., 2015). Therefore, preventing or controlling the clot formation in such cases is necessary. In a normal coagulation system, complex interactions of coagulation factors, platelets, cofactors, and regulators maintain homeostasis for the systematic regulation of bleeding and thrombus formation (Palta et al., 2014). The coagulation reaction has three pathways including the intrinsic pathway, the extrinsic pathway, and the common pathway (Gailani and Renné, 2007; Mackman et al., 2007). Among all the coagulation factors, thrombin (activated Factor II)—a glycosylated serine protease—is indispensable in the coagulation mechanism (Crawley et al., 2007; Smith et al., 2015). Its main function is to take charge of the most crucial and last step in the coagulation cascade reaction; the cleavage of fibrinogen and its activation into fibrin. Only then can fibrin bind to the glycoprotein IIb/IIIa receptor on platelets and connect with platelets and other coagulation factors to form a more solid clot in order to achieve hemostasis (Crawley et al., 2007). Therefore, targeting thrombin activity could be an effective strategy to control thrombosis. Heparin, argatroban, hirudin, and dabigatran are the commonly used anticoagulant drugs which

inhibit thrombin activity (Lee and Ansell, 2011; Alquwaizani et al., 2013). Heparin is one of the common anticoagulants in clinical treatment of pulmonary embolism, venous thrombosis, and cerebral embolism (Jin et al., 1997; Zhang et al., 2018). However, heparin may cause an immune-mediated coagulation side effect of heparin-induced thrombocytopenia (HIT) (Pollak et al., 2011). HIT causes abnormal coagulation of platelets and triggers thrombosis symptoms, and the incidence is higher for high-molecular-weight heparin than that of low-molecular-weight heparin. Therefore, developing an anticoagulant with high stability and low side effects is an important and challenging issue.

Aptamers are short DNA or RNA strands selected *in vitro* or *in vivo* through systematic evolution of ligands by exponential enrichment (SELEX) for strong and specific recognition of their targets (Darmostuk et al., 2015; Huang et al., 2016a; Lyu et al., 2016; Pang et al., 2018). In the past two decades, many aptamers have been selected to target different anticoagulation factors for anticoagulation applications (Pagano et al., 2008; Nimjee et al., 2016; Zavyalova et al., 2016a; Chabata et al., 2018). However, many of them suffer from poor specificity, weak binding strength and can be easily degraded by nucleases present in the blood, which limit their successful applications *in vivo*. Even so, a 15-mer thrombin-binding aptamer (TBA₁₅) with specific G-quadruplex structures, which can resist digestion by nucleases, has been shown to extend anticoagulation activity in whole blood (Bock et al., 1992). TBA₁₅ binds with thrombin (dissociation constant (K_d) of ~ 100 nM) at the fibrinogen-binding exosite I, resulting in the inhibition of thrombin activity (Padmanabhan et al., 1993). However, very high concentrations of TBA₁₅ (in micromolar regime) are required to achieve an appropriate anticoagulant response due to its low binding affinity. Another 29-mer thrombin-binding aptamer (TBA₂₉) exhibits much stronger binding with exosite II of thrombin ($K_d \sim 0.5$ nM) (Tasset et al., 1997); however, it could not

inhibit thrombin activity toward the formation of fibrin from fibrinogen and thrombin-mediated platelet activation. Moreover, the short half-life of blood circulation of TBAs diminishes their anticoagulation potency *in vivo*.

Compared to free aptamers, aptamer-conjugated nanoparticles provide ultrahigh local aptamer densities on nanoparticle surfaces to increase their binding affinity to thrombin and resistance toward nuclease digestion (Liu et al., 2014; Jo and Ban, 2016; Urmann et al., 2016; Yang et al., 2018). In addition, each nanoparticle can be conjugated with different functional aptamers for multivalent binding of target proteins. A number of TBA-based nanocomposites have been developed by modification of TBAs on metallic, polymeric, and DNA origami nanoparticles for efficient binding of TBAs with thrombin to increase their anticoagulation potency (Rinker et al., 2008; Kim et al., 2010; Musumeci and Montesarchio, 2012; Riccardi et al., 2017; Kumar and Seminario, 2018; Lai et al., 2018). However, anchoring of TBAs on the nanoparticles requires extensive and tedious functionalization processes. In addition, the steric position, distance, and orientation of TBAs on the nanoparticles are difficult to manipulate. Thus, these nanocomposites are rarely employed for anticoagulation *in vivo* (Lai et al., 2018).

Graphene oxide (GO) has been reported to adsorb single-stranded nucleic acid chains by cooperative van der Waals' force, π - π stacking interaction, and hydrogen bonding interaction (Antony and Grimme, 2008; Varghese et al., 2009; Wu et al., 2011; Chen et al., 2014; Liu et al., 2016). Recently, some aptamer-adsorbed GO have been demonstrated for protein detection and cell labeling (Pu et al., 2011; Gao et al., 2015; Kim et al., 2015; Xiao et al., 2017). Most aptamers adopt specific conformational structures, which enable high specificity toward the targeting molecule (Rowell et al., 1998; Tucker et al., 2012; Zavyalova et al., 2016b,c; Krauss et al., 2018). However, these unique conformational structures of aptamers are usually disrupted after adsorption onto GO. Moreover, the aptamer-adsorbed GO are not stable in human plasma due to the competitive adsorption between plasma components, such as high concentration proteins and aptamers on GO. As a result, the adsorbed aptamers tend to desorb from GO in human plasma (Wang et al., 2010; Mao et al., 2015; Zhu et al., 2015; Lu et al., 2016). In this study, we developed a simple strategy to target exosites I and II of thrombin simultaneously by using programmed hybrid-TBAs immobilized on partially reduced GO for enhanced stability of the TBAs and improved anticoagulation efficiency (Scheme 1). The targeting ligand is denoted as Supra-TBA_{15/29} [-(A₂₀h₁₅T₅TBA_{15/29}T₅h₁₅)_n-], containing a supramolecular structure of consecutive hybrid TBA₁₅/TBA₂₉ units with multiple poly(adenine) (A₂₀) segments for immobilization on GO. GO has been shown to preferentially interact with single stranded (ss) DNA with poly(adenine) sequences (Ranganathan et al., 2016). The multi-segment A₂₀ segments allow Supra-TBA_{15/29} to anchor strongly on the GO surface, which results in the high stability of Supra-TBA_{15/29}-GO nanocomposites in human plasma. The Supra-TBA_{15/29}-GO nanocomposites possess superior anticoagulant activity to free both TBAs (TBA₁₅ or TBA₂₉) and Supra-TBA_{15/29}. In addition, thromboelastography of whole-blood coagulation and rat-tail

bleeding assays further demonstrate the strong anticoagulation ability of Supra-TBA_{15/29}-GO (Graphical Abstract).

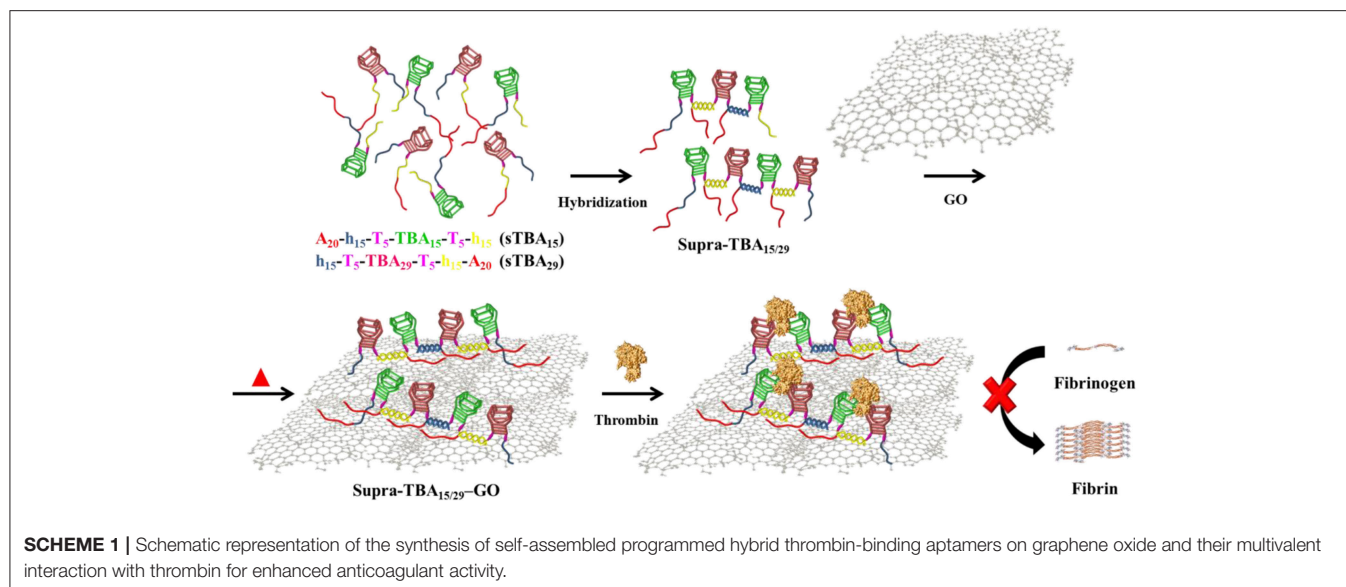
RESULTS AND DISCUSSION

Formation of Supra-TBA_{15/29}

The oligonucleotide sequences of A₂₀h₁₅T₅TBA₁₅T₅h₁₅ (sTBA₁₅) and h₁₅T₅TBA₂₉T₅h₁₅A₂₀ (sTBA₂₉) are listed in Table S1 (Supporting Information). The sTBA₁₅ and sTBA₂₉ comprised of three blocks, a 20-polyadenine (A₂₀) for anchoring on GO, two 15-base sequences (h₁₅) for consecutive hybridization, a 5-repeat thymidine (T₅) as a linker, and a TBA sequence providing functionality. TBA₂₉ has a G-quadruplex structure with a loop and stem in the terminal, while TBA₁₅ has only a G-quadruplex structure (Macaya et al., 1993; Padmanabhan et al., 1993). A previous study indicated that having two 7-mers inserted on each side of TBA₁₅ unit introduces a loop and stem structure for stabilizing the G-quadruplex structures, thereby increasing their inhibitory potency (Hsu et al., 2012). By simply mixing sTBA₁₅ and sTBA₂₉ in phosphate-buffered saline (PBS; containing 25.0 mM tris-HCl, 150.0 mM NaCl, 5 mM KCl, 1.0 mM MgCl₂, and 1.0 M CaCl₂; adjusted to pH 7.4 using HCl) solution, the Supra-TBA_{15/29} were formed through the consecutive hybridization of the h₁₅ sequences (Scheme S1A, Supporting Information). In addition, we also prepared dimer TBA₁₅/TBA₂₉ (di-TBA_{15/29}) by mixing sTBA₁₅ and dTBA₂₉ (nh₁₅T₅TBA₂₉T₅h₁₅A₂₀). The di-TBA_{15/29} are formed by a single step hybridization between sTBA₁₅ and dTBA₂₉ (Scheme S1B). A control experiment with a mixture of sTBA₁₅ and nTBA₂₉ (nh₁₅T₅TBA₂₉T₅nh₁₅A₂₀) indicated that they could not hybridize with each other (Scheme S1C). For simplicity, we denote the mixture of sTBA₁₅ and nTBA₂₉ as nh-TBA_{15/29}. The hydrodynamic size of Supra-TBA_{15/29} (~207.8 nm) was larger than sTBA₁₅ (~24.3 nm), sTBA₂₉ (~25.6 nm), di-TBA_{15/29} (~53.7 nm), and the mixture of sTBA₁₅ and nTBA₂₉ (~26.3 nm), determined by dynamic light scattering (DLS), which suggested the formation of a supramolecular TBA structure. The lower electrophoretic mobility of Supra-TBA_{15/29} compared to that of sTBA₁₅, sTBA₂₉, and di-TBA_{15/29} further confirmed the formation of Supra-TBA_{15/29} through hybridization (Figure S1, Supporting Information) (Hellman and Fried, 2007). The gel electrophoresis result of Supra-TBA_{15/29} shows a broad band, probably due to the formation of varying lengths of Supra-TBA_{15/29}. Based on the location and the width of the broad band, we propose that our Supra-TBA_{15/29} consists of mainly 2–6 hybridized TBA units.

Thrombin Clotting Time of Supra-TBA_{15/29}

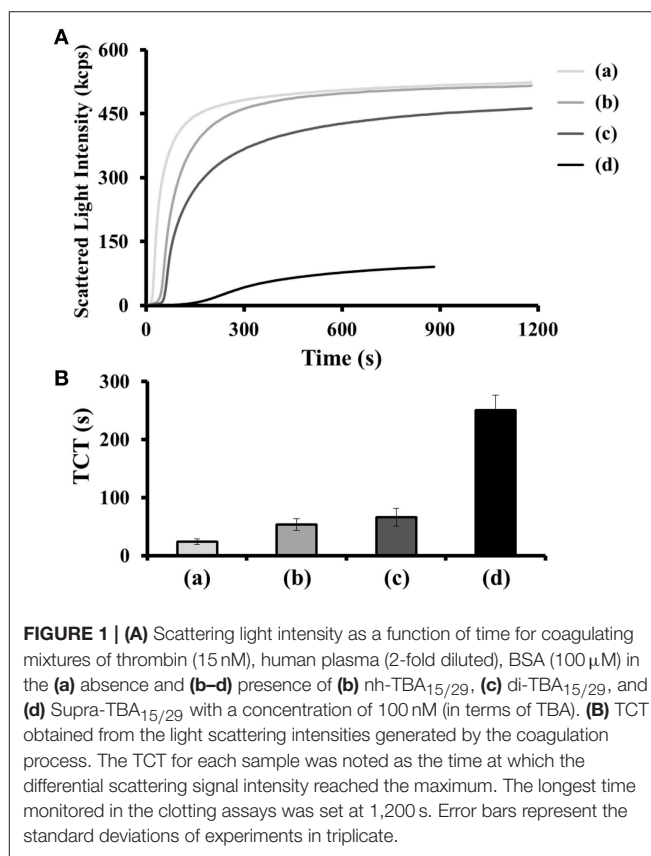
We evaluated the inhibitory ability of Supra-TBA_{15/29} against thrombin in human plasma by thrombin clotting time (TCT) assays. The TCT test is a reliable diagnostic tool for bleeding and/or clotting disorder and screening of coagulation factors I (fibrinogen), IIa (thrombin), and XIII (fibrinolysis stabilizing factor) in the common coagulation pathways (Ignjatovic, 2013). We investigated the thrombin inhibitory activity of nh-TBA_{15/29}, di-TBA_{15/29}, and Supra-TBA_{15/29}, which were prepared by mixing sTBA₁₅ with nTBA₂₉, dTBA₂₉, and sTBA₂₉ (Scheme S1),



respectively. We compared the inhibitory potencies of nh-TBA_{15/29}, di-TBA_{15/29}, and Supra-TBA_{15/29} by real-time kinetics of coagulation, through recording the scattering light intensity as a function of time (**Figure 1A**). Fibrinogen (factor I) is a fibrous glycoprotein (~45 nm) with a complex structure. It consists of three pairs of polypeptide chains (α -, β -, and γ -chains) linked together by 29 disulfide bonds (Mosesson, 2005). Soluble fibrinogen is converted into protofibrils by the cleavage of fibrinopeptides A α and B β in the central region by thrombin via intermolecular interactions of knobs “A” and “B” in the central nodule and holes “a” and “b” at the ends of the molecules. The protofibrils further aggregate laterally to form fibers and then branch to form a three-dimensional network of the fibrin clots. The higher activity of thrombin results in the formation of a larger fibrin gel, which causes increased scattering of light. The concentration of the total of the TBAs was held constant (100 nM) in these experiments. Compared with the control (no inhibitor), which has a TCT value of 24 ± 1 s, Supra-TBA_{15/29} prolonged the clotting time to 251 ± 21 s. The TCT values for nh-TBA_{15/29} and di-TBA_{15/29} were 54 ± 10 and 66 ± 15 s, respectively. The inhibitory activity of Supra-TBA_{15/29} was superior to nh-TBA_{15/29} and di-TBA_{15/29} mainly due to synergistic effect. That is, simultaneous binding and blocking by the two aptamers of both of the exosites (exosite I and II) of thrombin and steric hindrance of relatively large Supra-TBA_{15/29} to fibrinogen from accessing thrombin led to strong and synergistic inhibition of the thrombin-dependent coagulant activity (Hsu et al., 2011).

Characterization of GO and Supra-TBA_{15/29}-GO

GO was synthesized by improved Hummers’ method from graphite powder with a particle size of 7–11 μ m (Hummers and Offeman, 1958; Marcano et al., 2010). The detailed procedure of synthesis of GO is given in the experimental section. The TEM image in **Figure S2A** (Supporting Information) shows that



most of the as-synthesized GO with size ca. 200–300 nm are single layered. Atomic force microscopy (AFM) showed that the average size of a single-layer GO was ~230 nm, and the monolayer thickness was about 1.1 nm (**Figure S2B**, Supporting Information). We prepared a series of Supra-TBA_{15/29}-GO nanocomposites and studied their inhibitory activities against thrombin. The Supra-TBA_{15/29} ([TBA] = 2.5 μ M) was mixed

with GO (20–80 $\mu\text{g mL}^{-1}$) in PBS containing 1.0 M NaCl at 25–90°C. After incubation for 2 h, the Supra-TBA_{15/29}-GO solutions were purified through three centrifugation and washing cycles. The Supra-TBA_{15/29} on the GO was determined through the quantitation of unbound TBAs in the supernatant, and the results are listed in **Table S2**. The Supra-TBA_{15/29} modified on GO formed Supra-TBA_{15/29}-GO mainly through van der Waals' force, π - π stacking, and hydrogen-bonding between poly(adenine) (A₂₀) from Supra-TBA_{15/29} and GO (Antony and Grimme, 2008; Varghese et al., 2009; Chen et al., 2014). Previous studies revealed that purine bases (A and G) bind more strongly than the pyrimidines (T and C) (Park et al., 2014; Liu et al., 2016; Ranganathan et al., 2016). The DNA oligonucleotides possess much stronger [1–3 order(s) higher] association constants compared to the single nucleosides and longer DNA provides more binding sites for adsorption on GO. The AFM image of Supra-TBA_{15/29}-GO shows that Supra-TBA_{15/29} was anchored on the surface of GO with a thickness of \sim 16 nm (**Figure S2C**). The AFM result suggests a monolayer of Supra-TBA_{15/29} was immobilized on either side of the GO, which is evident from the size of TBA (\sim 2.0 nm) and the length of h₁₅T₅ (\sim 6.8 nm; 0.34 nm bp⁻¹).

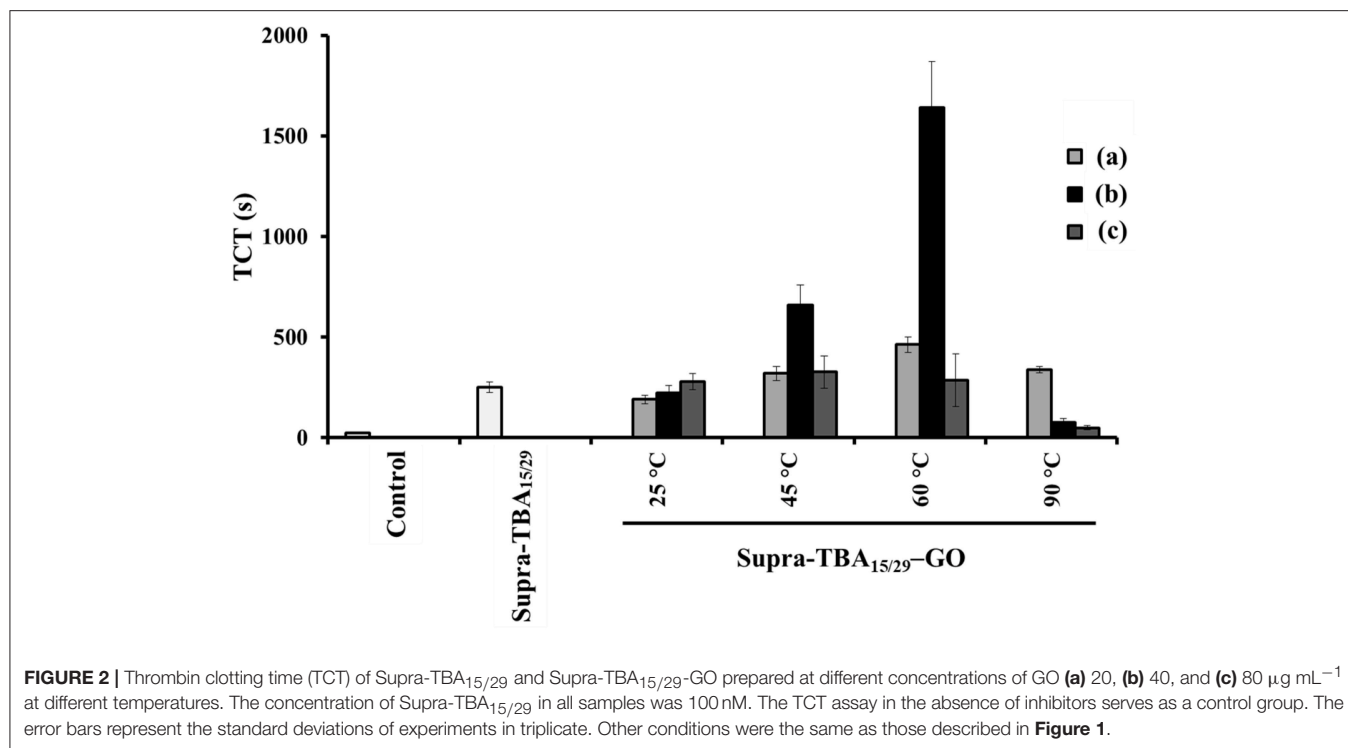
Temperature may affect the structure and flexibility of Supra-TBA_{15/29} and is known to affect oxygen moieties on GO, which in turn could affect their interactions during Supra-TBA_{15/29}-GO synthesis (Lin et al., 2010; Geggier et al., 2011; Brunet et al., 2018). Heat treatment altered the density of Supra-TBA_{15/29} on GO very significantly (**Table S2**) as a result of unfavorable entropy, partial denaturation of Supra-TBA_{15/29}, and mild reduction of GO at higher temperatures. The adsorption density of the Supra-TBA_{15/29} on GO decreased with increasing concentration of GO used during the preparation of Supra-TBA_{15/29}-GO conjugates. In the series of Supra-TBA_{15/29}-GO prepared, the maximum adsorption density of Supra-TBA_{15/29} on GO (using 20 $\mu\text{g mL}^{-1}$ of GO and at 25°C for the preparation of Supra-TBA_{15/29}-GO) was calculated to be 47.1 nmol mg⁻¹, which revealed a high density of Supra-TBA_{15/29} on the GO surface compared to the reported result for the saturated adsorption of poly-adenine (A₁₅) on GO (\sim 7.18 nmol mg⁻¹) (Lu et al., 2016). We conducted UV-vis absorption spectroscopy (**Figure S3**), Fourier-transform infrared spectroscopy (FT-IR; **Figure S4**), X-ray photoelectron spectroscopy (XPS; **Figure S5**), Raman spectroscopy (**Figure S6**), and elemental analysis (EA; **Table S2**) to characterize GO and understand the effect of temperature on the degree of reduction of GO. Our results indicate GO underwent only a slight reduction even after treatment at 90°C for 2 h. However, this slight reduction of GO played a crucial role in the anticoagulation potency and stability of Supra-TBA_{15/29}-GO in human plasma, which will be discussed in the following sections. The material is stored at 4°C when not in use and is stable up to 3 months.

Anticoagulant Activity of Supra-TBA_{15/29}-GO

In contrast to GO, which tends to aggregate in PBS of high ionic strength, the Supra-TBA_{15/29}-GO dispersion was very stable (no aggregation) when incubated in 1X PBS (**Figure S7**, Supporting

Information). The hydrodynamic size of GO aggregates in PBS was \sim 1,800 nm, whereas the size of Supra-TBA_{15/29}-GO (\sim 150 nm) did not change significantly with increasing the concentration of PBS. The high density of TBAs with high negative charge mainly contributed to the high stability of Supra-TBA_{15/29}-GO. On the other hand, the circular dichroism (CD) spectra of Supra-TBA_{15/29}-GO prepared at different temperatures (25–90°C) did not show significant difference with that of Supra-TBA_{15/29} (**Figure S8**, Supporting Information), revealing that the G-quadruplex structure of TBAs were highly preserved after Supra-TBA_{15/29} were adsorbed on GO. The TCT of Supra-TBA_{15/29} and Supra-TBA_{15/29}-GO prepared with various concentrations of GO (20, 40 and 80 $\mu\text{g mL}^{-1}$) at 25, 45, 60, and 90°C is presented in **Figure 2**. TCT values for Supra-TBA_{15/29}-GO prepared with GO (40 $\mu\text{g mL}^{-1}$) at 25, 45, 60, and 90°C were \sim 9, 26, 66, and three times longer, respectively, than that which was in the absence of inhibitor. The higher inhibitory activity of Supra-TBA_{15/29}-GO can be ascribed to the high specificity of the aptamers to block the exosite I and II binding sites and/or the active sites of thrombin for fibrinogen, and high ligand density on the GO surface. In addition, the 5' - and 3' -extended TBA molecules were anchored on GO through interactions between poly(adenine) and GO, which facilitated the exposure of major binding loops of TBA₁₅ (T³T⁴ and T¹²T¹³ loops) and TBA₂₉ (T¹⁰A¹¹ and T¹⁹T²⁰ loops) toward the bulk solution for access (binding) to thrombin. Previous reports revealed the binding of TBA₁₅ and TBA₂₉ to exosite I and exosite II of thrombin were through their T³T⁴/T¹²T¹³ loops and T¹⁰A¹¹/T¹⁹T²⁰ loops, respectively (Padmanabhan et al., 1993; Tasset et al., 1997).

The longest TCT time of $1,640 \pm 20$ s indicates that Supra-TBA_{15/29}-GO prepared with GO (40 $\mu\text{g mL}^{-1}$) at 60°C has the most significant impact on coagulation delay triggered by thrombin relative to the Supra-TBA_{15/29} and other Supra-TBA_{15/29}-GO nanocomposites. Although Supra-TBA_{15/29}-GO prepared in the lower temperature (<60°C) possess higher TBA density on GO (**Table S2**), the Supra-TBA_{15/29} tend to release from GO when incubated in human plasma due to the competitive interaction between high concentrated plasma components (e.g., serum albumin) and A₂₀ of Supra-TBA_{15/29} (**Figure S9**, Supporting Information) (Lu et al., 2016). We speculated that only a small portion of the A₂₀ of the highly dense Supra-TBA_{15/29} was adsorbed on GO and thus they were easily released from GO in complicated plasma. As a result, the anticoagulation ability was lower when the Supra-TBA_{15/29} were prepared at 25 and 40°C. On the other hand, the Supra-TBA_{15/29} probably disassembled when the Supra-TBA_{15/29}-GO was prepared at 90°C and resulted in much weaker anticoagulation activity than that of prepared at 60°C. The optimized Supra-TBA_{15/29}-GO prepared with GO (40 $\mu\text{g mL}^{-1}$) at 60°C exhibited the strongest inhibitory ability mainly due to an appropriate density, flexibility, and orientation of multivalent TBA on GO. All these factors are controllable by carefully controlling the concentration ratio of Supra-TBA_{15/29} to GO and reaction temperature, and thereby the interaction between Supra-TBA_{15/29} and GO. The appropriate orientation of the Supra-TBA_{15/29} on the slightly reduced GO surface



and the desired distance between TBA₁₅ and TBA₂₉ resulted in a superior multivalent binding. Compared with free TBA₁₅ ($K_d \sim 100$ nM) and TBA₂₉ ($K_d \sim 0.5$ nM) (Padmanabhan et al., 1993; Tasset et al., 1997), Supra-TBA_{15/29}-GO prepared with GO (40 μg mL⁻¹) at 60 °C exhibited much higher binding affinity toward thrombin ($K_d = 1.9 \times 10^{-11}$ M, **Figure S10**, Supporting Information). The Supra-TBA_{15/29}-GO prepared with GO (40 μg mL⁻¹) at 60 °C also exhibited superior anticoagulation activity compared to our previously reported bivalent TBA₁₅/TBA₂₉-modified gold nanoparticles and GO (Huang et al., 2016b; Lai et al., 2018), probably because the particular flexible conformation and multivalency of Supra-TBA_{15/29} structure on GO boosted their anticoagulation potency. A higher concentration of GO (80 μg mL⁻¹) for the preparation of Supra-TBA_{15/29}-GO prepared at 60 °C leads to lower aptamer density and lower local concentration on its surface, and lower concentration of GO (20 μg mL⁻¹) might cause steric hindrance for thrombin binding due to undesired conformation of highly dense aptamers on its surface. On the other hand, the Supra-TBA_{15/29}-GO prepared at 90 °C with 20 μg mL⁻¹ of GO exhibits a slightly better anticoagulant activity in comparison with that of 40 and 80 μg mL⁻¹ of GO. The slightly higher anticoagulant activity could be ascribed to the higher dense aptamers on the surface of GO with a concentration of 20 μg mL⁻¹ (**Table S2**, Supporting Information). The optimized Supra-TBA_{15/29}-GO prepared with GO (40 μg mL⁻¹) at 60 °C was used throughout the experiment.

The dose-dependent TCT displayed in **Figure 3** clearly demonstrates that optimized Supra-TBA_{15/29}-GO has the highest

inhibition of thrombin activity, in comparison with free Supra-TBA_{15/29} and the four tested commercial anticoagulant drugs including heparin, argatroban, hirudin, and warfarin. The TCT delay caused by Supra-TBA_{15/29}-GO ([TBA] = 100 nM) was 5, 10, 14, 37, and 40 times longer than that caused by the Supra-TBA_{15/29}, heparin, argatroban, hirudin, and warfarin (0.1 μM), respectively. The TCT assays clearly indicated that the clotting time delay by Supra-TBA_{15/29}-GO was much longer than that of Supra-TBA_{15/29} and the commercial anticoagulants. Our results reveal that Supra-TBA_{15/29}-GO is a stable and highly inhibitive nanocomposite for thrombin through elaborative construction of supramolecular TBA structures on the GO surface.

Thromboelastography

Platelets are tiny blood cell fragments that play an important role in blood clotting, including being activated to provide assembly sites for coagulation factor complex formation, combining with the fibrin clot and releasing agonists to amplify the platelet responses (De Candia, 2012). The evaluation of inhibition efficiency of Supra-TBA_{15/29}-GO by TCT assay has limitations, because they are conducted in plasma without platelets (thrombocytes). Therefore, we employed thrombin-activated thromboelastography (TEG) to study the kinetics of inhibition of clot formation in whole blood. Various parameters, such as the R time (time of latency from start of test to initial fibrin formation, amplitude of 2 mm), K time (time taken to achieve a certain level of clot strength, amplitude of 20 mm), α angle (measuring the speed at which fibrin build up and cross linking takes place), and MA (the ultimate strength of the fibrin clot) were measured using the TEG assay (Bolliger

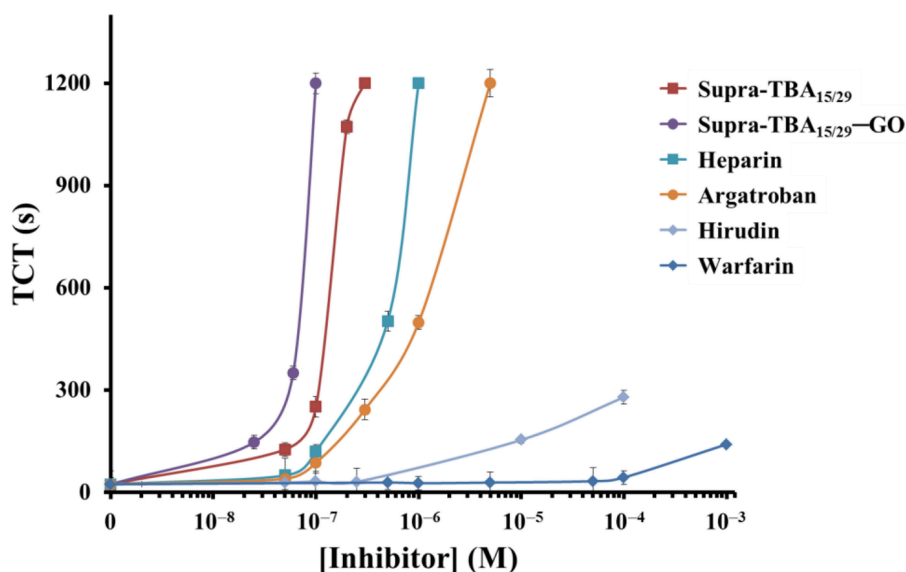


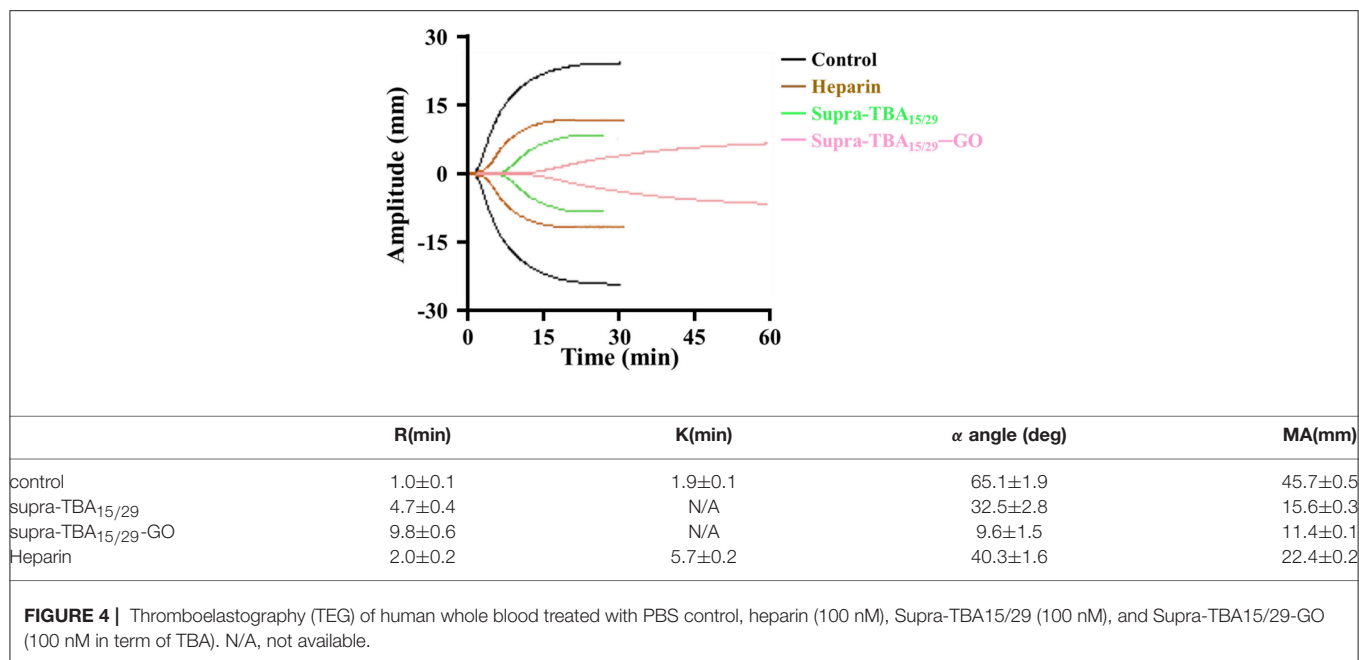
FIGURE 3 | Dose-dependence of the TCTs in human plasma in the presence of Supra-TBA_{15/29}, Supra-TBA_{15/29}-GO and commercial drugs heparin, argatroban, hirudin, and warfarin. The longest clotting assay time recorded was set at 1,200 s. Error bars represent the standard deviations of experiments in triplicate. Other conditions were the same as those described in **Figure 1**.

et al., 2012) to quantify the blood clot formation. As shown in **Figure 4**, Supra-TBA_{15/29} ([TBA] = 100 nM) prolonged the R time (4.7 ± 0.4 min) as compared with the control (without inhibitor) (1.0 ± 0.1 min), whereas Supra-TBA_{15/29}-GO prolonged the R value to 9.8 ± 0.6 min revealing that Supra-TBA_{15/29} exhibited a better inhibitory effect after it conjugated with GO. This result also indicates that Supra-TBA_{15/29}-GO in the whole blood sample can inhibit the coagulation pathway chain reaction more effectively than heparin (the most widely used anticoagulant) which prolonged the R value to 2.0 ± 0.2 min. Our results reveal that the anticoagulant activity of Supra-TBA_{15/29}-GO is about 5 times better than heparin in native human blood on the basis of R time values. Further, compared to the α angle, K time, and MA of Supra-TBA_{15/29} and heparin, Supra-TBA_{15/29}-GO has the longest K time and smallest α angle and MA values, indicating that the clot (fibrinogen polymerization and platelet aggregation) formed has the lowest rate and strength.

Biocompatibility

Carbon nanomaterials are reported to possess good biocompatibility (Seabra et al., 2014; Bhattacharya et al., 2016; Ou et al., 2016). Although GO has been shown to cause the rupture of cell membrane, the magnitude of decrease in cell viability does not exceed 20% for 24 h or even longer time when the concentration of GO is $<100 \mu\text{g mL}^{-1}$ (Liao et al., 2011; Fiorillo et al., 2015). Additionally, the cytotoxicity of GO is highly diminished after capping with biopolymers, such as proteins, oligonucleotide, and polysaccharide (Chong et al., 2015; Rezaei et al., 2016; Kenry, 2018; Liu et al., 2018; Ren et al., 2018). In this study, we used MTT assay to evaluate the

cytotoxicity of Supra-TBA_{15/29}-GO toward different mammalian cells (**Figure S11A**, Supporting Information). Supra-TBA_{15/29}-GO did not show any cytotoxic effect toward human lung adenocarcinoma epithelial cell (A549), human liver cancer cell (Hep-G2), human umbilical cord vein endothelial cell (HUVEC), and human embryonic kidney cell (HEK293T). The cells showed cell viability of $>95\%$ even at $1.00 \mu\text{M}$ (in terms of TBA) TBA_{15/29}-GO concentration and 24 h of incubation. It is noteworthy to mention that the concentration of Supra-TBA_{15/29}-GO used for MTT assay was several times higher than the effective concentration of Supra-TBA_{15/29}-GO used for antithrombin activity in plasma (**Figures 2, 3**) and whole blood (**Figure 4**). Live/dead cell viability staining (Calcein AM/EthD-1) was further employed for examining live and dead cells. Different concentrations of Supra-TBA_{15/29}-GO ([TBA] = 0.01 – $1.00 \mu\text{M}$) were added into a 24-well plate containing HEK293T cells. The morphologies of the HEK293T cells after 24 h culture with different Supra-TBA_{15/29}-GO concentrations showed no obvious differences when compared to the control (**Figure S11B**, Supporting Information). Supra-TBA_{15/29}-GO-treated cells were similar to that of the control group (PBS-treated only) which displayed typical fibroblast-like morphology (Yan and Shao, 2006). Calcein AM is a non-fluorescent dye that can easily permeate into live mammalian cells with an intact cell membrane. The hydrolysis of calcein AM by intracellular esterases produces calcein, which can be well-retained in the cell cytoplasm. Calcein exhibits strong green fluorescence at 520 nm upon excitation at 480–500 nm. EthD-1 cannot permeate through intact plasma membranes of live cells, but can enter cells with damaged cell membranes, and exhibits a strong red fluorescence (~ 40 -fold) at ~ 635 nm at excitation wavelengths



of 480–500 nm when it binds to nucleic acids in dead cells. The live/dead cell viability after calcein AM/EthD-1 staining further proved the low cytotoxicity of Supra-TBA_{15/29}-GO, with concentrations as high as 1.00 μ M and with green fluorescent cells predominating in the population (>98%). In addition, *in vitro* hemolysis experiments with defibrinated red blood cells (RBCs) did not show significant hemolysis for varying concentrations of Supra-TBA_{15/29}-GO (0–1.00 μ M; **Figure S12**, Supporting Information). Overall, our results reveal that Supra-TBA_{15/29}-GO has good biocompatibility and low cytotoxicity toward mammalian cells.

In vivo Rat-Tail Bleeding Assay

Tail-bleeding assay in rat was performed to understand the anti-hemostatic effect of Supra-TBA_{15/29}-GO *in vivo*. The rats (~200–250 g) were dosed (50 μ L/100 g) by intravenous injection with heparin (2.0 μ M), Supra-TBA_{15/29} (2.0 μ M), or Supra-TBA_{15/29}-GO (2.0 μ M) and waited for 5 min. Then, the rat tails were fully transected 4 mm from the tip. The control group of rats dosed with PBS had an average blood clot weight of 918.6 \pm 1.2 mg ($n = 5$), as shown in **Figure 5**. Compared with heparin, the Supra-TBA_{15/29}-GO-treated group showed superior anticoagulant effect. The blood clot weights of the Supra-TBA_{15/29}-GO-treated group (4,879 \pm 900 mg; $n = 5$) were significantly heavier than that of the control group ($P < 0.001$) and the heparin-treated group ($P < 0.05$). The body weights of the Supra-TBA_{15/29}-GO treated rats were almost the same as those of the untreated group ($P > 0.05$, $n = 5$) 10 days post-dose (data not shown). In addition, all Supra-TBA_{15/29}-GO treated rats survived for the next 2 months and exhibited normal behavior. The *in vivo* rat-tail bleeding assay study indicated that highly biocompatible Supra-TBA_{15/29}-GO possesses great potential as a safe and efficient

anticoagulant nanodrug for the treatment of thrombotic diseases, such as deep venous thrombosis, myocardial infarction, and thrombotic stroke.

CONCLUSIONS

In this study, highly stable and biocompatible supramolecular-aptamer functionalized GO nanosheets were prepared by a biomimetic approach. We successfully designed two different aptamers that can connectively hybridize and self-assemble on GO. AFM images showed that the Supra-TBA_{15/29}-GO was dispersed as 2D nanosheets. The Supra-TBA_{15/29}-GO was stable in high ionic strength solution as well as in human plasma. The structure of Supra-TBA_{15/29} on GO is controllable by mediating the ratio of Supra-TBA_{15/29} to GO and preparation temperature. The efficient inhibitory activity of Supra-TBA_{15/29}-GO against thrombin is due to precisely programmed TBA₁₅ and TBA₂₉'s hybridized structure on GO leading to strong interactions with thrombin and steric hindrance from fibrinogen substrate. The dose-dependent TCT delay caused by Supra-TBA_{15/29}-GO was >10 times longer than that of the most widely used anticoagulant heparin. In addition, the TEG and rat-tail bleeding experiment further proved the superior anticoagulant activity of Supra-TBA_{15/29}-GO relative to heparin. In the future, GO with small sizes may be employed for preparing Supra-TBA_{15/29}-GO to more efficiently reduce the uptake from the reticuloendothelial system in animals. In addition, various aptamers which target with different coagulation factors can be co-programmed on GO for systematic inhibition of multiple coagulation factors. Moreover, bioaccumulation, biopsy, metabolism, and acute and chronic toxicity should be conducted in animal models to confirm the

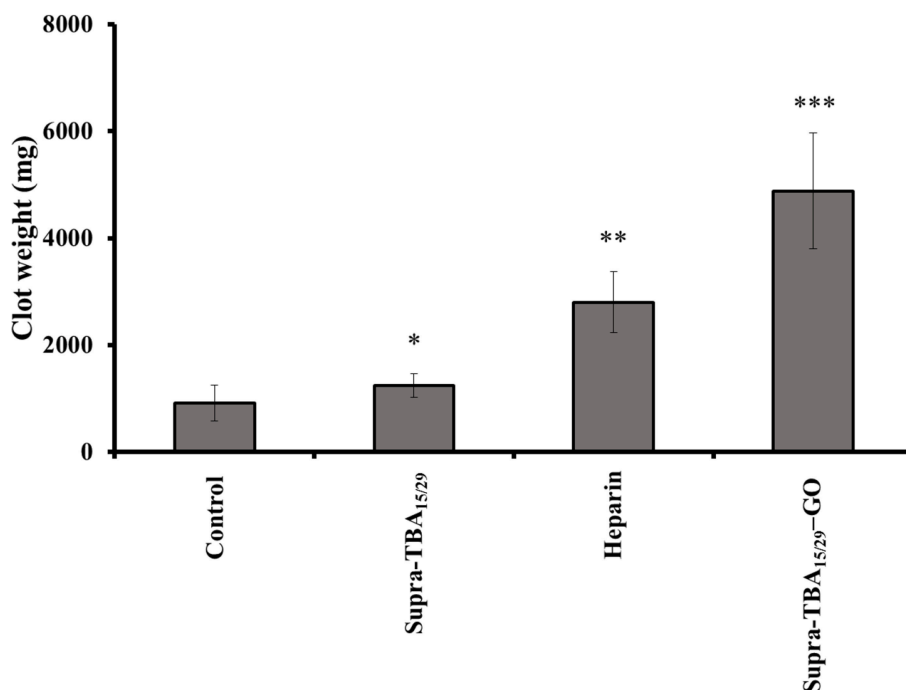


FIGURE 5 | The effect of Supra-TBA_{15/29}, heparin, and Supra-TBA_{15/29}-GO on rat-tail bleeding. Blood clots were collected after intravenous administration of the inhibitors (2.0 μ M, 100 μ L). Error bars represent the standard deviations of experiments in five rats. An asterisk indicates statistically significant differences (* P < 0.05, ** P < 0.01, *** P < 0.001; n = 5) as compared with the control group.

potential of supramolecular aptamer-GO nanocomposites as a safe and viable drug.

EXPERIMENTAL METHODS

Synthesis and Characterization of GO

GO was prepared by a modified Hummer's method (Hummers and Offeman, 1958; Marcano et al., 2010). Briefly, concentrated sulfuric acid (90 mL) and concentrated phosphoric acid (10 mL) were mixed and added to graphite powder (0.75 g) in a round bottomed flask. Potassium permanganate (4.50 g) was slowly added to the mixture and maintained at 50°C for 12 h with continuous stirring. Then, the reaction mixture was allowed to cool and placed in an ice bath, followed by slowly adding deionized water (100 mL) and hydrogen peroxide (32%) to the mixture until the solution turned from dark purple to bright yellow. The supernatant was removed by centrifugation at 35,000 g for 30 min. The residue was washed repeatedly with 5 mM sodium phosphate buffer (pH 7.4) until the solution pH was close to 7. The as-obtained graphite oxide was exfoliated by sonication for 2 h (power 200 W). The unoxidized graphite and large particles were separated at a relative centrifugal force (RCF) of 15,000 g for 30 min, and its weight/volume concentration was calculated by lyophilisation. An atomic force microscope (Shimadzu SPM-9600 AFM, Shimadzu Co, Kyoto, Japan) was used to analyze the size of GO. The dynamic light scattering (DLS) and zeta potential experiments were performed using a Zetasizer 3000HS analyzer (Malvern

Instruments, Malvern, UK). X-ray photoelectron spectroscopy (XPS) was performed using an ES-CALAB 250 spectrometer (VG Scientific, East Grinstead, UK) with Al K α X-ray radiation as the X-ray excitation source. Binding energies were corrected using the C1s peak at 284.8 eV as the standard. We also analyzed GO at different degrees of oxidation by using a DXR Raman microscope (Thermo Fisher Scientific Inc., Waltham, MA, USA) equipped with a 50X objective, a Nd:YAG laser (532 nm) and a charge-coupled detector. FT-IR spectroscopy was performed by using a Cary 640 FT-IR spectrometer (Santa Clara, CA, USA).

Synthesis of Supra-TBA_{15/29}-GO

A₂₀h₁₅T₅TBA₁₅T₅h₁₅ (sTBA₁₅) and h₁₅T₅TBA₂₉T₅h₁₅A₂₀ (sTBA₂₉) (2.5 μ M) were allowed to hybridize at 4°C for 1 h in PBS to form stable Supra-TBA_{15/29}. GO (40 μ g mL⁻¹) was added to the Supra-TBA_{15/29} and allowed to react. After 2 h of reaction, NaCl solution (1M) was added and maintained at 4°C for 1 h. Finally, the solution was heated to 25, 45, 60, and 90°C and kept for 1 h. The resulting solution was centrifuged at an RCF of 35,000 g for 2 h and the residues were resuspended with PBS. After three centrifugation and washing cycles, the amount of Supra-TBA_{15/29} adsorbed on GO was determined by quantitation of the un-adsorbed TBA in the supernatants by using Quanti-iT™ OliGreen ssDNA Reagent. The material was stored at 4°C when not in use and found to be stable for up to 3 months.

Thrombin Clotting Time (TCT) Assay

TCT tests for the common coagulation pathway were performed with nh-TBA_{15/29}, di-TBA_{15/29}, Supra-TBA_{15/29}, Supra-TBA_{15/29}-GO, and four commercial anticoagulants (heparin, argatroban, hirudin, and warfarin). Analytical solution containing PBS (pH 7.4), bovine serum albumin (100 μM), inhibitor (100 nM), and human plasma (2-fold diluted) was allowed to react for 15 min, maintained at 37°C for 3 min, and then mixed with thrombin (15 nM). Scattered light intensity at 650 nm was recorded using an FP-6500 spectrophotometer (JASCO, Tokyo, Japan). The TCT was noted as the time at which the differential scattering signal intensity reached the maximum. The measurements were done in triplicates, and a single batch of plasma was used for each set of experiments.

Thromboelastography

The anticoagulation efficiency of Supra-TBA_{15/29}, Supra-TBA_{15/29}-GO and heparin in whole blood clots was evaluated by thromboelastography (Haemoscope corporation, Niles, IL, USA), which measures the progress of blood clot formation and platelet-fibrin bond strength and monitors the internal interactions in blood and the contributions of cellular content. The plasma samples from healthy volunteers with were drawn from the vein, transferred to tubes containing sodium citrate, and immediately centrifuged at a relative centrifugal force (RCF) of 3000 g (10 min, 4°C). The human plasma collection procedure was approved by the Chang Gung Memorial Hospital institutional review board (IRB-103-6474A3) and informed consent was obtained from the volunteers prior to the collection of the plasma. Prior to the experiment, plain disposable plastic TEG cups (Haemonetics) were maintained at 37°C. In total, 52 μL of anticoagulant (0.5 μM) in PBS and 288 μL of whole blood were mixed in a TEG cup and incubated at 37°C for 10 min. To initiate the whole blood coagulation at 37°C, 20 μL of thrombin solution (270 nM) was added to the above mixture. The clot formation was recorded until a stable clot was formed or 1 h had passed. The various parameters, such as the reaction kinetics, α angle, and maximum amplitude were calculated using the TEG[®] Analytical Software version (TAS) 4.2.3 (Haemonetics).

Rat-Tail Bleeding Time

We used rat tail bleeding time to compare the anticoagulant effect of inhibitors *in vivo* in male rats of the Sprague Dawley (SD) strain weighing between 200 and 250 g. The experiments were conducted after getting permission from the Institutional Animal Care and Use Committee of the National Laboratory Animal Center (Permit number License No. IACUC106049). The rats

were anesthetized with Zoletil 50 with a dose of 100 μL/100 g body weight via subcutaneous injection. Supra-TBA_{15/29} (2 μM), Supra-TBA_{15/29}-GO (2 μM; in terms of TBA) or heparin (2 μM) was administered by intravenous injection at a dose of 50 μL/100 g, followed by waiting for 5 min. Then, 4 mm of the rat tail-tip was cut off, and the tail was immersed in PBS at 37°C. The blood clot weight until cessation of bleeding was determined.

Statistical Analysis

Student's *t*-test was performed and *P*-values < 0.05 were considered significant. The probability of rat survival was determined by the Kaplan–Meier method.

See the Supporting Information for the details on the materials, determination of the binding constant of thrombin with Supra-TBA_{15/29}-GO, *in vitro* cytotoxicity assays, and hemolysis assays.

ETHICS STATEMENT

The animal experiments were conducted after getting permission from the Institutional Animal Care and Use Committee of the National Laboratory Animal Center (Permit number License No. IACUC106049).

AUTHOR CONTRIBUTIONS

C-CH conceived the original idea, supervised the project from start to finish, and supervised the manuscript preparation. T-XL and P-XL carried out the experiments. J-YM and H-WC provided feedback, interpretation of the results, and helped with the preparation of the manuscript. BU and AA helped with manuscript preparation. All authors discussed the results and contributed to the manuscript.

ACKNOWLEDGMENTS

This study was supported by the Ministry of Science and Technology of Taiwan under Contract Nos. 107-2622-M-019-001-CC2, 104-2628-M-019-001-MY3, 107-2811-M-019-507, and 106-3114-8-019-002.

SUPPLEMENTARY MATERIAL

The Supplementary Material for this article can be found online at: <https://www.frontiersin.org/articles/10.3389/fchem.2019.00280/full#supplementary-material>

REFERENCES

- Alquwaizani, M., Buckley, L., Adams, C., and Fanikos, J. (2013). Anticoagulants: a review of the pharmacology, dosing, and complications. *Curr. Emerg. Hosp. Med. Rep.* 21, 83–97. doi: 10.1007/s40138-013-0014-6
- Antony, J., and Grimme, S. (2008). Structures and interaction energies of stacked graphene–nucleobase complexes. *Phys Chem. Chem. Phys.* 10, 2722–2729. doi: 10.1039/b718788b
- Bhattacharya, K., Mukherjee, S. P., Gallud, A., Burkert, S. C., Bistarelli, S., and Bellucci, S., et al. (2016). Biological interactions of carbon-based nanomaterials: from coronation to degradation. *Nanomed. Nanotechnol.* 12, 333–351. doi: 10.1016/j.nano.2015.11.011
- Bock, L. C., Griffin, L. C., Latham, J. A., Vermaas, E. H., and Toole, J. J. (1992). Selection of single-stranded DNA molecules that bind and inhibit human thrombin. *Nature.* 355, 564–566. doi: 10.1038/355564a0

- Bolliger, D., Seeberger, M. D., and Tanaka, K. A. (2012). Principles and practice of thromboelastography in clinical coagulation management and transfusion practice. *Transf. Med. Rev.* 26, 1–13. doi: 10.1016/j.tmr.2011.07.005
- Brunet, A., Salome, L., Rousseau, P., Destainville, N., Manghi, M., and Tardin, C. (2018). How does temperature impact the conformation of single DNA molecules below melting temperature? *Nucleic Acids Res.* 46, 2074–2081. doi: 10.1093/nar/gkx1285
- Chabata, C. V., Frederiksen, J. W., Sullenger, B. A., and Gunaratne, R. (2018). Emerging applications of aptamers for anticoagulation and hemostasis. *Curr. Opin. Hematol.* 25, 382–388. doi: 10.1097/MOH.0000000000000452
- Chen, J., Chen, L., Wang, Y., and Chen, S. (2014). Molecular dynamics simulations of the adsorption of DNA segments onto graphene oxide. *J. Phys. D Appl. Phys.* 47:505401. doi: 10.1088/0022-3727/47/50/505401
- Chong, Y., Ge, C., Yang, Z., Garate, J. A., Gu, Z., and Weber, J. K., et al. (2015). Reduced cytotoxicity of graphene nanosheets mediated by blood-protein coating. *ACS Nano* 9, 5713–5724. doi: 10.1021/nn5066606
- Crawley, J. T. B., Zanardelli, S., Chion, C. K. N. K., and Lane, D. A. (2007). The central role of thrombin in hemostasis. *J. Thromb. Haemost.* 5, 95–101. doi: 10.1111/j.1538-7836.2007.02500.x
- Darmostuk, M., Rimpelova, S., Gbelcova, H., and Ruml, T. (2015). Current approaches in SELEX: an update to aptamer selection technology. *Biotechnol. Adv.* 33, 1141–1161. doi: 10.1016/j.biotechadv.2015.02.008
- De Candia, E. (2012). Mechanisms of platelet activation by thrombin: a short history. *Thromb. Res.* 129, 250–256. doi: 10.1016/j.thromres.2011.11.001
- Doolittle, R. F. (2016). Some important milestones in the field of blood clotting. *J. Innate Immun.* 8, 23–29. doi: 10.1159/000442470
- Fiorillo, M., Verre, A. F., Iliut, M., Peiris-Pagés, M., Ozsvári, B., and Gandara, R., et al. (2015). Graphene oxide selectively targets cancer stem cells, across multiple tumor types: implications for non-toxic cancer treatment, via “differentiation-based nano-therapy.” *Oncotarget* 6, 3553–3562. doi: 10.18632/oncotarget.3348
- Gailani, D., and Renné, T. (2007). Intrinsic pathway of coagulation and arterial thrombosis. *Arterioscler. Thromb. Vasc. Biol.* 27, 2507–2513. doi: 10.1161/ATVBAHA.107.155952
- Gao, L., Li, Q., Li, R., Yan, L., Zhou, Y., Chen, K., et al. (2015). Highly sensitive detection for proteins using graphene oxide-aptamer based sensors. *Nanoscale* 7, 10903–10907. doi: 10.1039/c5nr01187f
- Geggy, S., Kotlyar, A., and Vologodskii, A. (2011). Temperature dependence of DNA persistence length. *Nucleic Acids Res.* 39, 1419–1426. doi: 10.1093/nar/gkq932
- Hellman, L. M., and Fried, M. G. (2007). Electrophoretic mobility shift assay (EMSA) for detecting protein–nucleic acid interactions. *Nat. Protoc.* 2, 1849–1861. doi: 10.1038/nprot.2007.249
- Hsu, C.-L., Chang, H.-T., Chen, C.-T., Wei, S.-C., Shiang, Y.-C., and Huang, C.-C. (2011). Highly efficient control of thrombin activity by multivalent nanoparticles. *Chem. Eur. J.* 17, 10994–11000. doi: 10.1002/chem.201101081
- Hsu, C.-L., Wei, S.-C., Jian, J.-W., Chang, H.-T., Chen, W.-H., and Huang, C.-C. (2012). Highly flexible and stable aptamer-caged nanoparticles for control of thrombin activity. *RSC Adv.* 2, 1577–1584. doi: 10.1039/c1ra00344e
- Huang, P.-J. J., Vazin, M., Lin, J. J., Pautler, R., and Liu, J. (2016a). Distinction of individual lanthanide ions with a DNAzyme beacon array. *ACS Sens.* 1, 732–738. doi: 10.1021/acssensors.6b00239
- Huang, S.-S., Wei, S.-C., Chang, H.-T., Lin, H.-J., and Huang, C.-C. (2016b). Gold nanoparticles modified with self-assembled hybrid monolayer of triblock aptamers as a photoreversible anticoagulant. *J. Control. Release.* 221, 9–17. doi: 10.1016/j.jconrel.2015.11.028
- Hummers, W. S. Jr., and Offeman, R. E. (1958). Preparation of graphitic oxide. *J. Am. Chem. Soc.* 80, 1339–1339. doi: 10.1021/ja01539a017
- Ignjatovic, V. (2013). Thrombin clotting time. *Methods Mol. Biol.* 992, 131–138. doi: 10.1007/978-1-62703-339-8_10
- Jin, L., Abrahams, J. P., Skinner, R., Petitou, M., Pike, R. N., and Carrell, R. W. (1997). The anticoagulant activation of antithrombin by heparin. *Proc. Natl. Acad. Sci. U.S.A.* 94, 14683–14688.
- Jo, H., and Ban, C. (2016). Aptamer–nanoparticle complexes as powerful diagnostic and therapeutic tools. *Exp. Mol. Med.* 48:e230. doi: 10.1038/emmm.2016.44
- Kenry (2018). Understanding the hemotoxicity of graphene nanomaterials through their interactions with blood proteins and cells. *J. Mater. Res.* 33, 44–57. doi: 10.1557/jmr.2017.388
- Kim, M.-G., Park, J. Y., Miao, W., Lee, J., and Oh, Y.-K. (2015). Polyaptamer DNA nanothread-anchored, reduced graphene oxide nanosheets for targeted delivery. *Biomaterials* 48, 129–136. doi: 10.1016/j.biomaterials.2015.01.009
- Kim, Y., Dennis, D. M., Morey, T., Yang, L., and Tan, W. (2010). Engineering dendritic aptamer assemblies as superior inhibitors of protein function. *Chem. Asian J.* 5, 56–59. doi: 10.1002/asia.200900421
- Krauss, I. R., Napolitano, V., Petraccone, L., Troisi, R., Spiridonova, V., and Mattia, C. A., et al. (2018). Duplex/quadruplex oligonucleotides: role of the duplex domain in the stabilization of a new generation of highly effective anti-thrombin aptamers. *Int. J. Biol. Macromol.* 107, 1697–1705. doi: 10.1016/j.ijbiomac.2017.10.033
- Kumar, N., and Seminario, J. M. (2018). Molecular dynamics study of thrombin capture by aptamers TBA26 and TBA29 coupled to a DNA origami. *Mol. Simul.* 44, 749–756. doi: 10.1080/08927022.2018.1448977
- Lai, P.-X., Mao, J.-Y., Unnikrishnan, B., Chu, H.-W., Wu, C.-W., and Chang, H.-T., et al. (2018). Self-assembled, bivalent aptamers on graphene oxide as an efficient anticoagulant. *Biomater. Sci.* 6, 1882–1891. doi: 10.1039/c8bm00288f
- Lee, C. J., and Ansell, J. E. (2011). Direct thrombin inhibitors. *Br. J. Clin. Pharmacol.* 72, 581–592. doi: 10.1111/j.1365-2125.2011.03916.x
- Liao, K.-H., Lin, Y.-S., Macosko, C. W., and Haynes, C. L. (2011). Cytotoxicity of graphene oxide and graphene in human erythrocytes and skin fibroblasts. *ACS Appl. Mater. Interfaces* 3, 2607–2615. doi: 10.1021/am200428v
- Lin, Z. Y., Yao, Y. G., Li, Z., Liu, Y., Li, Z., and Wong, C.-P. (2010). Solvent-assisted thermal reduction of graphite oxide. *J. Phys. Chem. C* 114, 14819–14825. doi: 10.1021/jp1049843
- Liu, B., Salgado, S., Maheshwari, V., and Liu, J. (2016). DNA adsorbed on graphene and graphene oxide: fundamental interactions, desorption and applications. *Curr. Opin. Colloid Interface Sci.* 26, 41–49. doi: 10.1016/j.cocis.2016.09.001
- Liu, Q., Jin, C., Wang, Y., Fang, X., Zhang, X., and Chen, Z., et al. (2014). Aptamer-conjugated nanomaterials for specific cancer cell recognition and targeted cancer therapy. *NPG Asia Mater.* 6:e95. doi: 10.1038/am.2014.12
- Liu, X., Cheng, X., Wang, F., Feng, L., Wang, Y., and Zheng, Y., et al. (2018). Targeted delivery of SNX-2112 by polysaccharide-modified graphene oxide nanocomposites for treatment of lung cancer. *Carbohydr. Polym.* 185, 85–95. doi: 10.1016/j.carbpol.2018.01.014
- Lu, C., Huang, P.-J. J., Liu, B., Ying, Y., and Liu, J. (2016). Comparison of graphene oxide and reduced graphene oxide for DNA adsorption and sensing. *Langmuir* 32, 10776–10783. doi: 10.1021/acs.langmuir.6b03032
- Lyu, Y., Chen, G., Shangguan, D., Zhang, L., Wan, S., and Wu, Y., et al. (2016). Generating cell targeting aptamers for nanotheranostics using cell-SELEX. *Theranostics* 6, 1440–1452. doi: 10.7150/thno.15666
- Macaya, R. F., Schultze, P., Smith, F. W., Roe, J. A., and Feigon, J. (1993). Thrombin-binding DNA aptamer forms a unimolecular quadruplex structure in solution. *Proc. Natl. Acad. Sci. U.S.A.* 90, 3745–3749.
- Mackman, N., Tilley, R. E., and Key, N. S. (2007). Role of the extrinsic pathway of blood coagulation in hemostasis and thrombosis. *Arterioscler. Thromb. Vasc. Biol.* 27, 1687–1693. doi: 10.1161/ATVBAHA.107.141911
- Mao, Y., Chen, Y., Li, S., Lin, S., and Jiang, Y. (2015). A graphene-based biosensing platform based on regulated release of an aptameric DNA biosensor. *Sensors* 15, 28244–28256. doi: 10.3390/s151128244
- Marcano, D. C., Kosynkin, D. V., Berlin, J. M., Sinitiskii, A., Sun, Z., and Slesarev, A., et al. (2010). Improved synthesis of graphene oxide. *ACS Nano* 4, 4806–4814. doi: 10.1021/nn1006368
- Morfini, M., Coppola, A., Franchini, M., and Di Minno, G. (2013). Clinical use of factor VIII and factor IX concentrates. *Blood Transf.* 11, S55–S63. doi: 10.2450/2013.0105
- Mosesson, M. W. (2005). Fibrinogen and fibrin structure and functions. *J. Thromb. Haemost.* 3, 1894–1904. doi: 10.1111/j.1538-7836.2005.01365.x
- Musumeci, D., and Montesarchio, D. (2012). Polyvalent nucleic acid aptamers and modulation of their activity: a focus on the thrombin binding aptamer. *Pharmacol. Ther.* 136, 202–215. doi: 10.1016/j.pharmthera.2012.07.011
- Nimjee, S. M., Povsic, T. J., Sullenger, B. A., and Becker, R. C. (2016). Translation and clinical development of antithrombotic aptamers. *Nucl. Acid Ther.* 26, 147–155. doi: 10.1089/nat.2015.0581

- Otsuka, F., Yasuda, S., Noguchi, T., and Ishibashi-Ueda, H. (2016). Pathology of coronary atherosclerosis and thrombosis. *Cardiovasc. Diagn. Ther.* 6, 396–408. doi: 10.21037/cdt.2016.06.01
- Ou, L., Song, B., Liang, H., Liu, J., Feng, X., and Deng, B., et al. (2016). Toxicity of graphene-family nanoparticles: a general review of the origins and mechanisms. *Part. Fibre Toxicol.* 13:57. doi: 10.1186/s12989-016-0168-y
- Padmanabhan, K., Padmanabhan, K. P., Ferrara, J. D., Sadler, J. E., and Tulinsky, A. (1993). The structure of α -thrombin inhibited by a 15-mer single-stranded DNA aptamer. *J. Biol. Chem.* 268, 17651–17654.
- Pagano, B., Martino, L., Randazzo, A., and Giancola, C. (2008). Stability and binding properties of a modified thrombin binding aptamer. *Biophys. J.* 94, 562–569. doi: 10.1529/biophysj.107.117382
- Palta, S., Saroa, R., and Palta, A. (2014). Overview of the coagulation system. *Indian J. Anaesth.* 58, 515–523. doi: 10.4103/0019-5049.144643
- Pang, X., Cui, C., Wan, S., Jiang, Y., Zhang, L., and Xia, L., et al. (2018). Bioapplications of cell-SELEX-generated aptamers in cancer diagnostics, therapeutics, theranostics and biomarker discovery: a comprehensive review. *Cancers*. 10:E47. doi: 10.3390/cancers10020047
- Park, J. S., Goo, N.-I., and Kim, D. E. (2014). Mechanism of DNA adsorption and desorption on graphene oxide. *Langmuir*. 30, 12587–12595. doi: 10.1021/la503401d
- Pollak, U., Yacobovich, J., Tamary, H., Dagan, O., and Manor-Shulman, O. (2011). Heparin-induced thrombocytopenia and extracorporeal membrane oxygenation: a case report and review of the literature. *J. Extra. Corpor. Technol.* 43, 5–12.
- Previtali, E., Bucciarelli, P., Passamonti, S. M., and Martinelli, I. (2011). Risk factors for venous and arterial thrombosis. *Blood Transf.* 9, 120–138. doi: 10.2450/2010.0066-10
- Pu, Y., Zhu, Z., Han, D., Liu, H., Liu, J., and Liao, J., et al. (2011). Insulin-binding aptamer-conjugated graphene oxide for insulin detection. *Analyst*. 136, 4138–4140. doi: 10.1039/c1an15407a
- Rana, K., and Neeves, K. B. (2016). Blood flow and mass transfer regulation of coagulation. *Blood Rev.* 30, 357–368. doi: 10.1016/j.blre.2016.04.004
- Ranganathan, S. V., Halvorsen, K., Myers, C. A., Robertson, N. M., Yigit, M. V., and Chen, A. A. (2016). Complex thermodynamic behavior of single-stranded nucleic acid adsorption to graphene surfaces. *Langmuir*. 32, 6028–6034. doi: 10.1021/acs.langmuir.6b00456
- Ren, X., Li, J., Chen, C., Gao, Y., Chen, D., and Su, M., et al. (2018). Graphene analogues in aquatic environments and porous media: dispersion, aggregation, deposition and transformation. *Environ. Sci. Nano*. 5, 1298–1340. doi: 10.1039/c7en01258f
- Rezaei, A., Akhavan, O., Hashemi, E., and Shamsara, M. (2016). Toward chemical perfection of graphene-based gene carrier via Ugi multicomponent assembly process. *Biomacromolecules*. 17, 2963–2971. doi: 10.1021/acs.biomac.6b00767
- Riccardi, C., Krauss, I. R., Musumeci, D., Morvan, F., Meyer, A., and Vasseur, J.-J., et al. (2017). Fluorescent thrombin binding aptamer-tagged nanoparticles for an efficient and reversible control of thrombin activity. *ACS Appl. Mater. Interfaces*. 9, 35574–35587. doi: 10.1021/acsami.7b11195
- Rinker, S., Ke, Y., Liu, Y., Chhabra, R., and Yan, H. (2008). Self-assembled DNA nanostructures for distance dependent multivalent ligand–protein binding. *Nat. Nanotechnol.* 3, 418–422. doi: 10.1038/nnano.2008.164
- Rowell, S., Stonehouse, N. J., Convery, M. A., Adams, C. J., Ellington, A. D., and Hirao, I., et al. (1998). Crystal structures of a series of RNA aptamers complexed to the same protein target. *Nat. Struct. Biol.* 5, 970–975. doi: 10.1038/2946
- Seabra, A. B., Paula, A. J., de Lima, R., Alves, O. L., and Durán, N. (2014). Nanotoxicity of graphene and graphene oxide. *Chem. Res. Toxicol.* 27, 159–168. doi: 10.1021/tx400385x
- Smith, S. A., Travers, R. J., and Morrissey, J. H. (2015). How it all starts: initiation of the clotting cascade. *Crit. Rev. Biochem. Mol. Biol.* 50, 326–336. doi: 10.3109/10409238.2015.1050550
- Suppiej, A., Gentilomo, C., Saracco, P., Sartori, S., Agostini, M., and Bagna, R., et al. (2015). Paediatric arterial ischaemic stroke and cerebral sinovenous thrombosis. *Thromb. Haemost.* 113, 1270–1277. doi: 10.1160/TH14-05-0431
- Tasset, D. M., Kubik, M. F., and Steiner, W. (1997). Oligonucleotide inhibitors of human thrombin that bind distinct epitopes. *J. Mol. Biol.* 272, 688–698. doi: 10.1006/jmbi.1997.1275
- Tucker, W. O., Shum, K. T., and Tanner, J. A. (2012). G-quadruplex DNA aptamers and their ligands: structure, function and application. *Curr. Pharm. Design.* 18, 2014–2026. doi: 10.2174/138161212799958477
- Urmann, K., Modrejewski, J., Scheper, T., and Walter, J.-G. (2016). Aptamer-modified nanomaterials: principles and applications. *BioNanoMaterials*. 18, 1–2. doi: 10.1515/bnm-2016-0012
- Varghese, N., Mogera, U., Govindaraj, A., Das, A., Maiti, P. K., and Sood, A. K., et al. (2009). Binding of DNA nucleobases and nucleosides with graphene. *ChemPhysChem*. 10, 206–210. doi: 10.1002/cphc.200800459
- Wang, Y., Li, Z., Hu, D., Lin, C.-T., Li, J., and Lin, Y. (2010). Aptamer/graphene oxide nanocomplex for *in situ* molecular probing in living cells. *J. Am. Chem. Soc.* 132, 9274–9276. doi: 10.1021/ja103169v
- Wu, M., Kempaiah, R., Huang, P.-J. J., Maheshwari, V., and Liu, J. (2011). Adsorption and desorption of DNA on graphene oxide studied by fluorescently labeled oligonucleotides. *Langmuir*. 27, 2731–2738. doi: 10.1021/la1037926
- Xiao, K., Liu, J., Chen, H., Zhang, S., and Kong, J. (2017). A label-free and high-efficient GO-based aptasensor for cancer cells based on cyclic enzymatic signal amplification. *Biosens. Bioelectron.* 91, 76–81. doi: 10.1016/j.bios.2016.11.057
- Yan, W., and Shao, R. (2006). Transduction of a mesenchyme-specific gene periostin into 293T cells induces cell invasive activity through epithelial-mesenchymal transformation. *J. Biol. Chem.* 281, 19700–19708. doi: 10.1074/jbc.M601856200
- Yang, Y., Yang, X., Yang, Y., and Yuan, Q. (2018). Aptamer-functionalized carbon nanomaterials electrochemical sensors for detecting cancer relevant biomolecules. *Carbon*. 129, 380–395. doi: 10.1016/j.carbon.2017.12.013
- Zavalyova, E., Golovin, A., Pavlova, G., and Kopylov, A. (2016a). Development of antithrombotic aptamers: from recognizing elements to drugs. *Curr. Pharm. Design.* 22, 5163–5176. doi: 10.2174/1381612822666161004163409
- Zavalyova, E., Tagiltsev, G., Reshetnikov, R., Arutyunyan, A., and Kopylov, A. (2016b). Cation coordination alters the conformation of a thrombin-binding G-quadruplex DNA aptamer that affects inhibition of thrombin. *Nucl. Acid Ther.* 26, 299–308. doi: 10.1089/nat.2016.0606
- Zavalyova, E., Ustinov, N., Golovin, A., Pavlova, G., and Kopylov, A. (2016c). G-quadruplex aptamers to human thrombin versus other direct thrombin inhibitors: the focus on mechanism of action and drug efficiency as anticoagulants. *Curr. Med. Chem.* 23, 2230–2244. doi: 10.2174/0929867323666160517120126
- Zhang, Z., Li, Z., Li, J., and Liu, L. (2018). Effects of natural hirudin and low molecular weight heparin in preventing deep venous thrombosis in aged patients with intertrochanteric fracture. *Sci. Rep.* 8:8847. doi: 10.1038/s41598-018-27243-1
- Zhu, Y., Cai, Y., Xu, L., Zheng, L., Wang, L., and Qi, B., et al. (2015). Building an aptamer/graphene oxide FRET biosensor for one-step detection of bisphenol A. *ACS Appl. Mater. Interfaces*. 7, 7492–7496. doi: 10.1021/acsami.5b00199

Conflict of Interest Statement: The authors declare that the research was conducted in the absence of any commercial or financial relationships that could be construed as a potential conflict of interest.

Copyright © 2019 Lin, Lai, Mao, Chu, Unnikrishnan, Anand and Huang. This is an open-access article distributed under the terms of the Creative Commons Attribution License (CC BY). The use, distribution or reproduction in other forums is permitted, provided the original author(s) and the copyright owner(s) are credited and that the original publication in this journal is cited, in accordance with accepted academic practice. No use, distribution or reproduction is permitted which does not comply with these terms.